Adaptive Cruise Control Euro NCAP validation using CLF-CBF and Model-Free control law in CarSim

Fernando Z. Preto * **Mateus M. Brugnolli** * **Bruno A. Angélico** *

* *Applied Control Laboratory LCA of Escola Politécnica - University of São Paulo, Brazil, (e-mails: [zolubas,mateus_mmb,angelico]@usp.br)*

Abstract:
Safety critical embedded algorithms such as ACC (adaptive cruise control) must be validated rigorously to grant safety. Therefore, this paper presents a realistic validation of an ACC control architecture focused on safety according to the standard protocol Euro NCAP Test. The control implementation is a cascade closed loop control. The upper level controller is a quadratic programming framework based on a CLF (Control Lyapunov Function) to ensure cruise speed control with a CBF (Control Barrier Function) to ensure safety. The lower level controller is a model-free control to ensure that the solution could be applied to any vehicle, since this approach is based on an ultra-local model obtained online. Additionally, the constraints for the CLF-CBF parameters are derived to ensure that the ACC system meets practical performance standards. The proposed ACC was able to accomplish Euro NCAP tests, as demonstrated in CarSim/Simulink simulations.

Keywords:
Adaptive Cruise Control, ACC, Advanced Driver Assistance Systems, ADAS, Control Lyapunov Function, CLF, Control Barrier Function, CBF, Model-Free control, CarSim, Euro NCAP, RADAR.

1. INTRODUCTION

The Adaptive Cruise Control (ACC) is an Advanced Driver Assistance Systems (ADAS) functionality designed to provide safety and convenience by partially automating the driving task of maintaining highway cruising speed. This is a popular functionality developed long ago by many manufacturers according to Marsden et al. (2001).

Since then, modern control approaches explicitly focused on safety, such as Control Barrier Functions (CBF), have been proposed (Ames et al., 2019). However, to the best of the author's knowledge, there are no published results yet that validate an ACC system on trustworthy automotive simulators according to standard test protocols.

Therefore, this work uses the mathematically proven safety of CBF combined with Control Lyapunov Functions (CLF) for an ACC system design. Here, the convergence of the host vehicle speed to the desired cruise speed acts as a soft constraint, while the safety is guaranteed using a hard constraint, as performed by Ames et al. (2017). However, since CLF-CBF model-based control depends on a mathematical model of the vehicle, the usage of a complex model can compromise the real-time properties ensured by Quadratic Programming (QP) solvers. To avoid this problem, this work considers the proposal of Chinelato et al. (2023) for a closed-loop cascade control where the Upper level control is a framework based on CLF-CBF powered by QP and the lower level control is a model-free control (Fliess and Join, 2013).

The model-free control is based on an ultra-local model obtained online that handles strong nonlinear dynamics using feedback linearization. In this way, this lower level control ensures that the control architecture of Figure 1 could be implemented in any automobile, provided that the vehicle mass and approximate information about the aerodynamics are known. This will be discussed in the Modeling Section.

It is important to note that some numerical values used in parameter fitting were deliberately chosen to showcase the algorithm's behavior under critical conditions. However, more robust values could be selected to ensure safety.

The main contributions of this work are the derivation of constraint formulas for the CLF-CBF parameters to ensure practical performance, and the validation of compliance with Euro NCAP tests (Euro NCAP, 2020). The proposed ACC system is validated using CarSim and Matlab/Simulink realistic simulation, demonstrating the approach as a functional and safe strategy to be implemented by the automotive industry.

The work is organized as follows: Section 2 presents the control law architecture and the vehicle modeling. Section 3 discusses the CBF design and its tuning feasibility conditions. Next, Section 4 presents the CLF design and its tuning. The complete CLF-CBF framework and its QP implementation are presented in Section 5. The lower level controller, model-free control, is shown in Section 6, including its design and tuning. Section 7 explores the feasibility conditions. Finally, Section 8 shows the Carsim

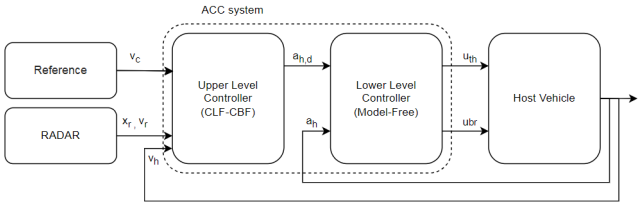

Figure 1. ACC Control Architecture. Adapted from Naus et al. (2010)

Euro NCAP validation results and Section 9 presents the conclusions of the work.

2. SYSTEM MODELING AND CONTROL

2.1 Control Law Architechture

In Figure 1, v_c is the reference cruising speed of the road, D is the distance between the host vehicle and the leader vehicle, v_r is the relative speed related to the previous distance D. According to the CLF-CBF control, $a_{h,d}$ is the desired acceleration of the host, a_h is the actual acceleration of the host, and v_h is the host speed. Next, the model-free control imposes u_{th} as the acceleration pedal and u_{br} as the brake pedal signal.

The upper level controller is a CLF-CBF control law that grants stability, performance, safety, and comfort. The lower level controller is a model-free control that tracks the CLF-CBF control reference and deals with highly complex vehicle dynamics such as gear changes, suspension, and tire effects to impose the desired acceleration on the vehicle and allows the simple model (Equation (2)) to be enough for the CLF-CBF formulation to work in practice.

2.2 Vehicle Modeling

From the upper level perspective, consider the state of the vehicle as $x = [v_h \ D]'$, where D is the distance between the host and the leader vehicle. Note that the speed of a leader vehicle on the road v_ℓ acts as a model disturbance, not a model state. Then, a nonlinear model for the host vehicle is (2) with the general form of Equation (1).

$$\dot{x} = f(x) + g(x)u \tag{1}$$

$$\begin{bmatrix} \dot{v}_h \\ \dot{D} \end{bmatrix} = \underbrace{\begin{bmatrix} -\dfrac{F_r(v_h)}{M} \\ v_\ell - v_h \end{bmatrix}}_{f(x)} + \underbrace{\begin{bmatrix} 1 \\ 0 \end{bmatrix}}_{g(x)} u \tag{2}$$

where M is the vehicle mass and $F_r(v_h)$ is the net force dependent on the host speed. This force is an empirical model of the drag generated by the air and other no modeled effects. It is adopted $F_r(v_h) = f_0 + f_1 v_h + f_2 v_h^2$ as in (Ames et al., 2017) with f_0, f_1, f_2 fitted empirically.

3. CBF: CONTROL BARRIER FUNCTION

The CBF control is commonly used to grant that states will be invariant to a safe set $\mathcal{C}$. For the implementation of embedded systems, the preferred formulation is ZCBF (Zeroing Control Barrier Function) since it has limited values (Ames et al., 2017).

3.1 ACC ZCBF Design and Tuning

In terms of states $x = [v_h, D]$, the ACC safety condition is

$$\frac{D}{v_h} \geq T_d \tag{3}$$

where D/v_h is the time headway of the host vehicle referenced to the measurement point P at the leader vehicle position, as shown in Figure 2. Michael et al. (2000) states that it is impossible to remain safe following with time headway T_d smaller than 2s. Other countries adopt different values such as the "half the speedometer rule" in Germany, which leads to $T_d = 1.8$s (Vogel, 2003). One of the most cited papers in the field adopted $T_d = 2.5$s (Li et al., 2011). This paper considers $T_d = 2$ s, but in our experience, we recommend selecting higher values to grant safety.

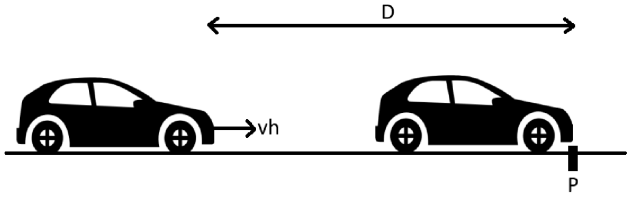

Figure 2. Time Headway.

Rearranging (3) leads to zeroing barrier candidate (4) which implies in the safe state set $\mathcal{C}$ defined in (5). The safe set is defined in (6), where $\partial\mathcal{C}$ refers to the boundary of the safe set $\mathcal{C}$ and $\text{Int}(\mathcal{C}) = \mathcal{C} - \partial\mathcal{C}$. Note that $h(x)$ is not a function of v_ℓ since CBF is only a function of the states x. Nonetheless, the CBF-based control depends on v_ℓ in B.2, then this variable is not ignored.

$$h(x) := D - T_d v_h \tag{4}$$

$$\mathcal{C} = \{x = [v_h, D] : D - T_d v_h \geq 0\} \tag{5}$$

$$\begin{cases} \mathcal{C} = \{x \in \mathbb{R}^n : h(x) \geq 0\} \\ \partial\mathcal{C} = \{x \in \mathbb{R}^n : h(x) = 0\} \\ \text{Int}(\mathcal{C}) = \{x \in \mathbb{R}^n : h(x) > 0\} \end{cases} \tag{6}$$

The next step to grant safety is to prove that zeroing barrier candidate h defined in (4) leads to feasible ZCBF, since feasible ZCBF implies forward invariance of set $\mathcal{C}$ according to Ames et al. (2017).

Proposition 1. *If $h(x)$ zeroing barrier defined in (4) was a feasible ZCBF for all admissible control $u \in \mathcal{U}$, then the proposed ACC will grant the safety condition (3).*

The proof sketch for Proposition 1 is described in Appendix B.

Considering (B.4) and (18) with $u^{\min} = a^{\min}$, a proposed formula to fit $\gamma > 0$ to maintain ACC safety condition is

$$\gamma^{\max} = \frac{T_d u^{\min} + v_h^{\max} - \dfrac{T_d F_r(v_h^{\max})}{M}}{-\dfrac{(v_h^{\max})^2}{2u^{\min}} - T_d v_h^{\max}} \tag{7}$$

Note that $\gamma^{\max}$ is the limit condition to safety, that is, one designing an ACC based on the proposed method should select $\gamma \ll \gamma^{\max}$ to ensure safety as a priority. Note that γ should not be too close to zero since the vehicle will always travel slowly compared to v_c in this case.

4. CLF: CONTROL LYAPUNOV FUNCTION

According to Ames et al. (2017), CLF guarantees the stability and exponential convergence of the states of system (1) to desired states. In the case of ACC, this is used to ensure that the host vehicle will reach the desired cruising speed v_c. Note that normally, a Lyapunov function should not be defined in terms of only one state (Slotine and Li, 1991). However, since stability was previously granted in the hard constraint given by CBF, then one can consider this CLF based only on state v_h to track the reference v_c when condition (8) is satisfied.

4.1 ACC CLF Design and Tuning

The CBF grants that the states $x = [v_h \ D]'$ are stable in the meaning of the Nagumo's invariant sets theorems. When condition (8) is satisfied, it is desirable that v_h converges fast to v_c. And when condition (9) is verified, then $v_h = vc$ must be relaxed to maintain the safety requirement $D > 0$. The arbitration between ensuring condition (8) or relaxing it is implemented as explored by Ames et al. (2017) using a CLF defined only to the convergence of the state v_h given that CBF grants $D \in \mathcal{C}$.

$$[v_c \ D]' \in \mathcal{C} \tag{8}$$

$$[v_c \ D]' \notin \mathcal{C} \tag{9}$$

A candidate Lyapunov function $V(v_h)$ such that the system is stabilized around the reference v_c is

$$V(v_h) := (v_h - v_c)^2 \tag{10}$$

Defined $V(v_h)$ candidate, the next necessary step is to prove the proposition 2 to ensure that CLF is capable to granting $v_h \to v_c$ when (8).

Proposition 2. *If the CLF based on $V(v_h)$ was feasible for all admissible control $u \in \mathcal{U}$, then the proposed controller based on this CLF will grant fast convergence of v_h to v_c when controlling the system (1) and* (8) *was verified.*

The proof sketch for Proposition 2 is described in Appendix A.

The parameter c_V defines the exponential convergence of the system to the reference (Chinelato et al., 2023). Then one must choose c_V as large as possible to grant fast convergence to the target, but limited to $c_V \in C_R$. However, one could desire that the system become more aggressive in following the v_c reference, which requires the choice $c_V > \sup C_R$, where sup is the supremum of a set. In this case, CLF still works as discussed in Section 7.3, nevertheless, the main difference compared to the proof development of Proposition 2 is that the control will saturate until the required control effort is smaller than the limits of $\mathcal{U}$.

5. CLF-CBF FRAMEWORK

This section introduces the CLF-CBF framework. Based on the CLF and CBF described in Sections 4 and 3 respectively, the quadratic programming (QP) is used to unite the two control objectives and carry out the arbitration between performance and security requirements, always prioritizing security. Based on the framework proposed by Ames et al. (2017), QP seeks to minimize the following control effort

$$u^*(x) = \min_{\mathbf{u}=(u,\delta)\in\mathbb{R}^{m+1}} \frac{1}{2} u^T H(x) u + F(x)^T u \tag{11}$$

$$\begin{cases} s.t. \\ \text{Stability \& Tracking: } A_{CLF} u \leq b_{CLF} \\ \text{Safety: } A_{CBF} u \leq b_{CBF} \\ \text{Comfort: } A_{COM} u \leq b_{COM} \end{cases} \tag{12}$$

Where

$$\begin{cases} H = 2 \begin{bmatrix} \frac{1}{M^2} & 0 \\ 0 & p_{sc} \end{bmatrix}, F = -2 \begin{bmatrix} \frac{F_r(v_h)}{M^2} \\ 0 \end{bmatrix} \\ A_{CLF} = [L_g V(x), -1] \\ b_{CLF} = -L_f V(x) - c_V V(x) \\ A_{CBF} = [-L_g h(x), 0] \\ b_{CBF} = L_f h(x) + \gamma h(x) \\ A_{COM} = \begin{bmatrix} 1 & 0 \\ -1 & 0 \end{bmatrix}, b_{COM} = \begin{bmatrix} a_{\text{accel}}^{\max} \\ a_{\text{brake}}^{\max} \end{bmatrix} \end{cases} \tag{13}$$

According to the model described in Section 2.2, the CLF constraints are $A_{CLF} = [2(v_h - v_d), -1]$, $b_{CLF} = \frac{-2F_r(v_d - v_h)}{M} - c_V(v_h - v_d)^2$. The CBF constraints are $A_{CBF} = [-Td, 0]$, $b_{CBF} = (v_\ell - v_h + \frac{F_r \cdot Td}{M}) + \gamma(D - Td \cdot v_h)$. And the comfort constraints are $a_{\text{accel}}^{\max} = a_{\text{brake}}^{\max} = |a^{\min}|$ (see Table 1). The p_{sc} is the weight of Lyapunov's relaxation δ that makes CLF a soft constraint and CBF a hard constraint, as described by Ames et al. (2017).

To solve the proposed QP problem, the algorithm proposed by Hildreth (1957) was chosen because it is suitable for embedded applications.

6. MODEL-FREE CONTROL

The model-free control is used as a lower level control in the proposed ACC system. This approach uses a feedback linearization with the estimated model online. In other words, this control law allows the model (2) to be suitable for the host vehicle, since more complex dynamics terms are attenuated by this method.

6.1 Resumed theoretical background

The model-free control (Fliess and Join, 2013) is a control law based on an ultra-local model in the form (14) that is estimated online. In the case of the ACC system, the controlled variable is the speed y and the model (14) is an algebraic estimator for $\dot{y}$

$$\dot{y} = \Phi + \alpha u \tag{14}$$

where Φ is a constant value at each short period of time T that represents the unknown non-linear dynamics of the system and α is a gain that means how the control effort u affects $\dot{y}$.

A control law that cancels the dynamics of the ultra-local model (14) is (15) where $\hat{\Phi}$ is an online identified parameter that approximates Φ, $\hat{\alpha}$ offline fitted gain that approximate α, and y^* is the desired trajectory.

$$u = -\frac{\hat{\Phi} - \dot{y^*} - \text{PID}(e)}{\hat{\alpha}} \tag{15}$$

Note that applying control effort (15) to (14) leads to (16), assuming $\hat{\alpha} \approx \alpha$ and $\hat{\Phi} \approx \Phi$. This means that the non-linear unknown system modeled by (14) now has exponential reference tracking governed by a simple PID control. That would be the main advantage of the model-free control applied to highly complex dynamical systems.

This is possible because $\hat{\Phi}$ is calculated by (17) where a discrete trapezoidal approximation can be considered with $T = NT_s$, where T_s is the sampling time assuming Zero-Order Holder and N is the number of samples to be measured to estimate Φ in the short period T. Equation (17) is obtained by transforming (14) in Laplace domain, then applying $\frac{d}{ds}$ operator in (14) to eliminate constants, then multiplying (14) by s^{-2} to eliminate derivative terms and impose at least a first order integration in each term, and finally applying the Laplace anti-transform.

$$\dot{e} = -\text{PID}(e) \tag{16}$$

$$\hat{\Phi} = -\frac{6}{T^3}\int_0^T (T - 2\tau)y(\tau)\,d\tau - \frac{6\alpha}{T^3}\int_0^T (T\tau - \tau^2)u(\tau)\,d\tau. \tag{17}$$

Sections 6.2, 6.3, 6.4 and 6.5 show how to empirically fit the model-free control parameters using simulations in a reliable environment like the CarSim simulator.

6.2 Fit of parameter α

The consequence of having $\hat{\alpha} \neq \alpha$ is that the cancelation of dynamics (14) by (15) is not exact. In addition, if the fraction $\hat{\alpha}/\alpha$ is greater than 1, the PID(e) gains will be greater than desired and the model-free control will be more aggressive than desired. If this fraction is less than 1, the opposite will happen. Fine-tuning can be achieved by a simple step response of the system.

6.3 Fit of parameter T_s

The sampling time should be fitted empirically, ensuring that T_s is short enough to be possible to have at least N samples to perform (17) in a short time T such as ultra-local model assumption to remain valid.

6.4 Fit of parameter N

The N is fitted empirically. If N is too small, then the integrative filter of (17) will not filter noise of u and y properly and $\hat{\Phi}$ will not be representative of Φ. Conversely, if N is too big then ultra-local model assumption in T is no longer valid.

6.5 Fit PID

Proportional-Integral-Derivative controllers are designed to be heuristically fitted. In the present work, we used CarSim simulator to have reliable vehicle data to fit the PID according to Garcia (2017).

7. FEASIBILITY CONDITIONS

The following section is a discussion about some feasibility aspects related to ACC design to pass on the Euro NCAP Protocol Tests.

7.1 Breaking capacity condition

The Euro NCAP (2020) considers that an ACC algorithm should have deceleration limited to $a^{\min} = -5\text{m/s}^2$. Thus, Torricelli's equation $V^2 = V_0^2 + 2a\Delta S$ leads to the feasibility condition of relative distance, $D^{\min}$, such that it is still possible to break the host traveling at $v_h^{\max}$ without colliding with the stopped leader vehicle ($v_\ell = 0$) and respecting $a^{\min}$. Rearranging Torricelli's equation with $V = 0$, $V_0 = v_\ell = v_h^{\max}$, $a = a^{\min}$, $\Delta S = D^{\min}$ then (18) shows the minimum RADAR's required range.

$$D^{\min} = -\frac{(v_h^{\max})^2}{2a^{\min}} \tag{18}$$

7.2 RADAR

The maximum allowed speed on the road considered in this paper is $v_h^{\max} = 130\text{km/h}$. Thus (18) implies $D^{\min} = 130.4$. Note that $D_{\text{RADAR}} = 140\text{m}$ is a critical choice, since only approximately 10m was adopted as a relaxation compared to the minimum feasible value $D^{\min}$.

The RADAR's required field of view (FoV) must primarily consider the traffic lane width. However, it is possible to have situations where smaller elements are detected, like motorcycles. Considering Euro NCAP (2020) CCRS - Curved road test, Figure 3 indicates the geometric reference for the FoV design. Considering traffic lane width $\overline{DC} = 3.5\text{m}$, $\overline{AB} = D_{\text{RADAR}} = 140\text{m}$, $\overline{DB} = \overline{DC}/2$ then the minimum FoV to the VUT be able to detect the GVT2 must be $\theta^{\min} = \arcsin(\frac{\overline{DB} + \overline{DC}}{\overline{AB}}) \approx \pm 3°$. However, given the narrower profile of motorcycles compared to cars, a better and adopted choice is FoV $\theta = \pm 7.5°$.

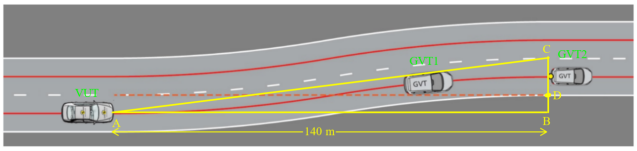

Figure 3. Adapted from CCRS - Curved road test Euro NCAP (2020)

7.3 Saturation on accelerator

For the parameters of Table 1, $\sup C_R \approx 0.28$, but we design a more aggressive system with $c_V = 0.8$. Thus, one can see in Figure 9 that the control signal $a_{h,d}$ keeps saturated in the time interval $t \in [0, 5.5]\text{s}$ until it starts to decrease. And this occurs at this time because approximating (A.5) by $u_{\max} \approx -\frac{c_V e}{2} = 5\text{m/s}^2$ one can see that if the absolute value of the tracking error is $\geq 45\text{km/h}$, then the control signal $a_{h,d}$ saturates. And at $5,5\text{s}$ the error is in fact $v_h - v_c \approx -45\text{km/h}$ in Figure 9. Then, Figure 9 shows that CLF works under control saturation condition.

7.4 CBF Recovery Policy

The forward invariance of the states $x \in \mathcal{C}$ is only granted by CBF if the system starts with $h(x) > 0$. However, some tests of Euro NCAP (2020) start with the $h < 0$. Thus, a recovery barrier policy must be used. And the

only reasonable policy is to force acceleration reference $a_{h,d} = a^{\min}$ until the CBF becomes positive again. With this policy, the safeness was granted in the tests of the section 8.

8. EURO NCAP TESTS

The complete description of the tests is in Euro NCAP (2020). The protocol shows numerous tests. Only one of each category is then described in detail to illustrate the proposed behavior of the ACC system. Following the protocol nomenclature, the lead vehicle is called GVT (Global Vehicle Target) and the host vehicle with ACC is called VUT (Vehicle Under Test).

8.1 Numerical tuning

Table 1. Parameters of the System

Description	Parameter	Value
Adopted Headway	T_d	2
Mass	M	1500 kg
Drag coefficient	f_0	0.1
Drag coefficient	f_1	5
Drag coefficient	f_2	0.25
QP weight	p_{sc}	100
CLF Convergence	c_V	0.8
CBF Safety	γ	0.00005
Sampling Time	T_s	0.02
Number of Samples	$N = N^{\text{Accel}} = N^{\text{Brake}}$	50
Model-Free gain	K_p^{Accel}	5
Model-Free gain	α^{Accel}	4
Model-Free gain	K_p^{Brake}	15
Model-Free gain	α^{Brake}	100
RADAR's Range	D_{RADAR}	140 m
RADAR's FoV	θ	$\pm 7.5°$
Euro NCAP (2020)	$a^{\min}$	-5m/s^2

In the Table 1 some parameters were chosen to explore the limits of the proposed algorithm. These parameters are T_d, that should be chosen greater to enhance safeness level, c_V that should be chosen smaller to avoid control saturations and D_{RADAR} that should be chosen greater to enhance the capability of the system to detect problematic leader vehicles with time enough to avoid accidents under a smooth braking scenario.

Note that for the values in Table 1, $\gamma^{\max} \approx 0.43$, nevertheless we selected $\gamma \approx \gamma^{\max} 10^{-4}$ to ensure safety during the hardest tests of the Euro NCAP protocol, so evaluating whether γ is close to zero is not a trivial task and requires a realistic and trusted simulation environment to fit a functional γ value.

8.2 Used notation and general comments

For all following presented tests, v_c is the reference cruising speed, v_ℓ is the GVT speed measured by the VUT's RADAR, v_h is the VUT speed, D is the relative distance between VUT and GVT measured by the VUT's RADAR, $a_{h,d}$ is the acceleration/braking reference form upper-level controller and a_h is the VUT's acceleration after the lower-level controller and actuators to have acted on the VUT.

For all following simulations, it is possible to see that the VUT's deceleration a_h has some overshooting, but this is acceptable according to the Euro NCAP (2020). Note that the absolute value of $a_{h,d}$ is maintained always lower than 5m/s^2.

And again for all the following simulations, when the RADAR has no detections, the distance is assumed as its maximum value D_{RADAR} and the GVT speed is assumed as $v_l = v_c$.

8.3 CCRS – STATIONARY TARGET

The test conditions are GVT: $v_\ell = 0\text{km/h}$; VUT: $v_c \in [70, 130]\text{km/h}$.

This test consists of 7 subtests. Each test is shown in Figure 5 by a strip, white, or green. For each test, the VUT is required to reach a speed v_c and then brake because there is a stopped GVT on the road. Figure 5 shows that the barrier function $h(x)$ is always positive during the initial six tests. In the seventh test, the barrier is lost, but recovered in time adopting the strategy discussed in Section 7.4. Figure 4 shows the CarSim environment simulation in which the vehicles do not collide at the end of the seventh CCRS test.

Figure 4. CCRS - Straight Road test. CarSim.

8.4 CCRM – MOVING TARGET

The test conditions are GVT: $v_\ell = 20\text{km/h}$; VUT: $v_c \in [80, 130]\text{km/h}$. Figure 6 shows this test results. The interpretation of the results is similar to the CCRS test with the difference that the speed of the GVT is now 20km/h.

8.5 CCRB – BRAKING TARGET

The test conditions are GVT: $v_\ell = 50\text{km/h}$ breaking at -6m/s^2; VUT: $v_c = 55\text{km/h}$. The initial relative distance is 12m. Figure 7 shows this test results. Note this test is extremely severe since the initial distance is too small and the deceleration of GVT is 1m/s^2 greater than the maximum allowed deceleration for the VUT. In terms of CBF, the initial conditions of this Euro NCAP's test force the barrier to start at a barrier breach condition $h < 0$. Thus, the only thing that the system could do without using emergence braking algorithms is saturated the braking action, that is what is observed in $a_{h,d}$ in the time interval $t \in [67, 70]\text{s}$ after that the barrier is recovered $h \geq 0$.

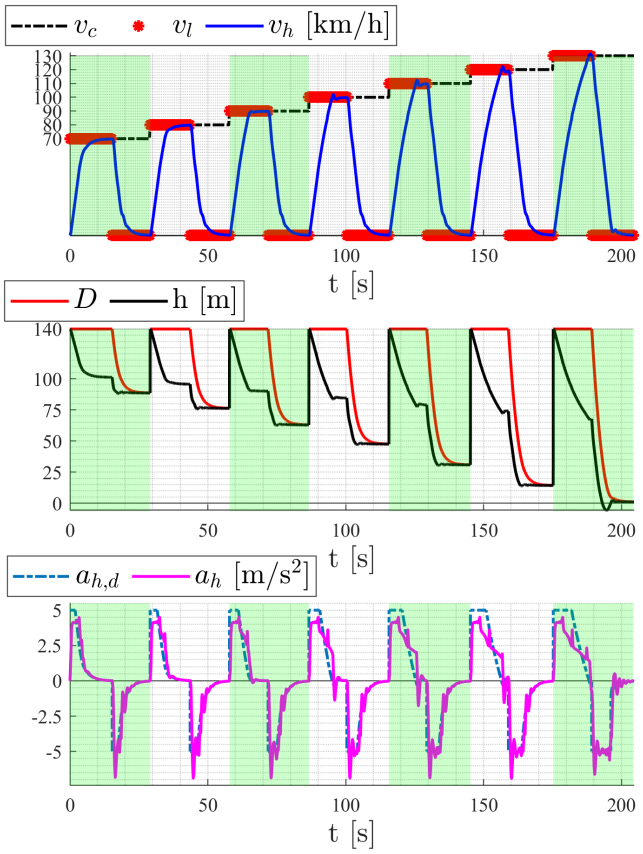

Figure 5. CCRS - Straight Road test. Speeds, accelerations, Distance and CBF h.

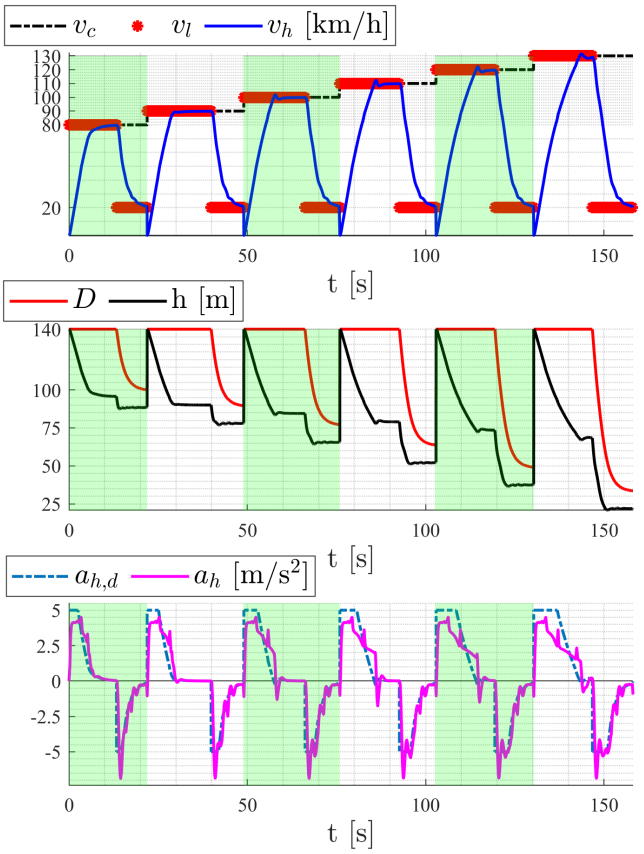

Figure 6. CCRM with GVT at 20km/h: Accelerations.

8.6 CUT-IN

The test conditions are GVT: v_ℓ = 70km/h; VUT: v_c = 120km/h. The initial time to collision is TCC= 1.5s. Figure 8 and 9 show this test in five frames. From left to right, the white GVT vehicle changes dangerously its traffic lane to the blue VUT's traffic lane. And the VUT's speed is 120km/h while GVT's speed is only 70km/h. Thus, the VUT brakes until the barrier h stops to decrease granting safety.

8.7 CUT-OUT

The test conditions are GVT: v_ℓ = 70km/h; VUT: v_c = 90km/h. The initial time to collision is TCC= 3s. Figures 10 and 11 show this test in five frames. From left to right, the blue GVT vehicle travels faraway from VUT $D > D_{\text{RADAR}}$, then blue GVT is detected travelling at 70km/h and VUT brakes softly in the time interval $t \in [18, 22]$s, then blue GVT changes its traffic lane to the left lane and VUT stops to detect vehicles in front of it, then VUT start to detect the white GVT that is stopped on the road and finally the VUT brakes hardly until stops at a safe distance from the white GVT. In the Figure 11 one interesting behavior happens at t = 23s, the CBF saturates the breaking with $h \geq 0$ since the γ was chosen to be very rigorous to maintain safety. In other words, it is possible to see the CBF acting without the intervention of the CBF recovery police discussed in the section 7.4.

9. CONCLUSIONS

This article presents a model-based control strategy that employs CLF and CBF to leverage model-free control in the design of an ACC system capable of maintaining the desired cruise speed while ensuring safety. Additionally, this paper offers a comprehensive understanding of the parameters of the proposed ACC algorithm, with a particular focus on the CLF-CBF parameters design and the RADAR's parameter selection. All of these aspects were implemented in the trusted Simulink-CarSim simulation environment, thus validating the proposed ACC in accordance with the Euro NCAP Test protocol 2020.

ACKNOWLEDGMENTS

Authors would like to thank Fundação de Desenvolvimento da Pesquisa - Fundep Rota 2030 - Linha V for the Grant SEGCOM, Fundação de Amparo à Pesquisa do Estado de São Paulo - FAPESP, Grant 2023/04628-6, and Coordenação de Aperfeiçoamento de Pessoal de Nível Superior - Brasil (CAPES), Finance Code 001.

REFERENCES

Ames, A.D., Coogan, S., Egerstedt, M., Notomista, G., Sreenath, K., and Tabuada, P. (2019). Control barrier functions: Theory and applications. In *2019 18th European Control Conference (ECC)*, 3420–3431.

Ames, A.D., Xu, X., Grizzle, J.W., and Tabuada, P. (2017). Control barrier function based quadratic programs for safety critical systems. *IEEE Transactions on Automatic Control*, 62(8), 3861–3876.

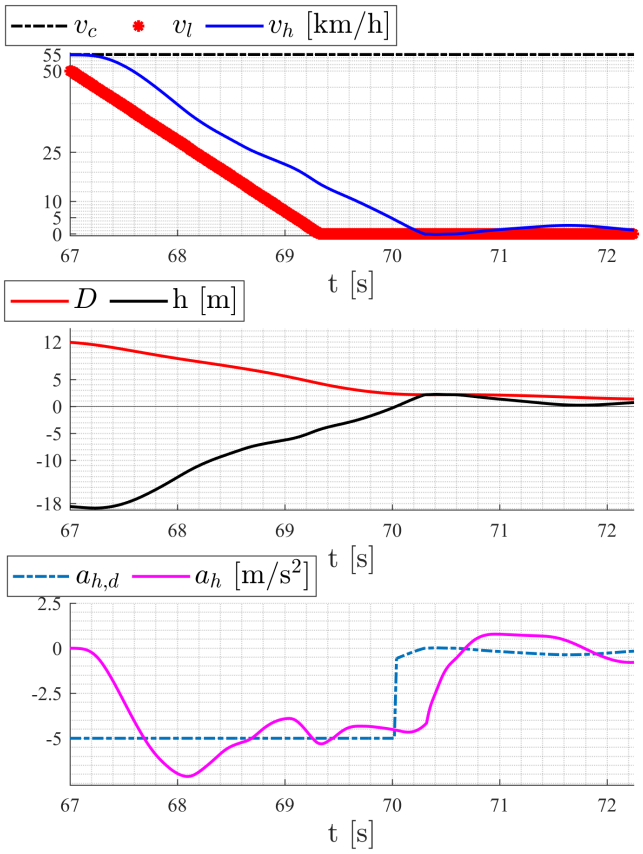

Figure 7. CCRB with GVT braking at 6m/s^2 with 12m of relative distance between GVT and VUT: Accelerations.

Figure 8. CUT-IN: CarSim simulation.

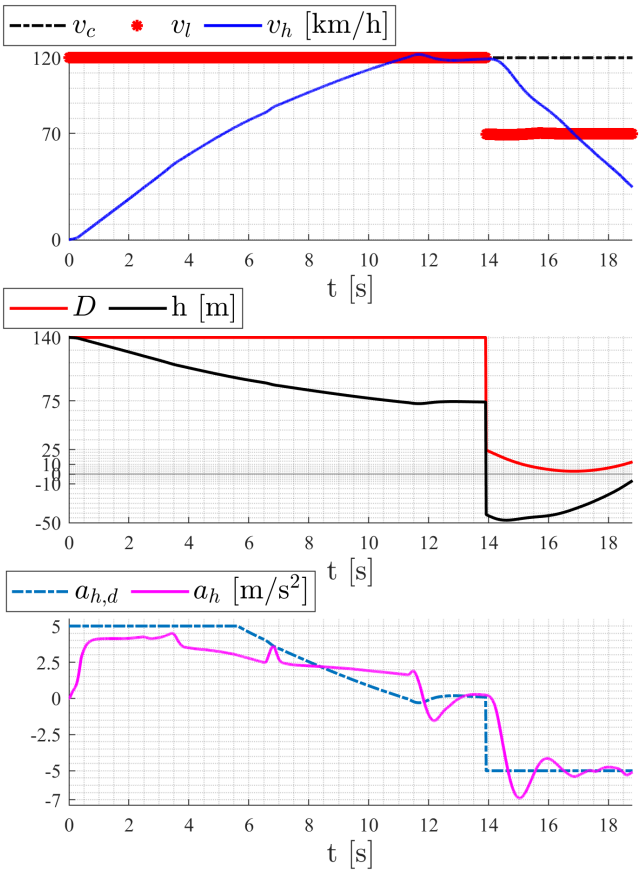

Figure 9. CUT-IN: Accelerations.

Figure 10. CUT-OUT: Accelerations.

Chinelato, C.I.G., Angélico, B.A., Justo, J.F., and Laganá, A.A.M. (2023). Design of adaptive cruise control with control barrier function and model-free control. *Journal of Control, Automation and Electrical Systems*, 34(3), 470–483.

Euro NCAP (2020). The European New Assessment Programme (Euro NCAP). URL `https://www.euroncap.com/en`. Accessed: March, 2022.

Fliess, M. and Join, C. (2013). Model-free control. *International Journal of Control*, 86(12), 2228–2252.

Garcia, C. (2017). *Controle de Processos Industriais. Estratégias Convencionais*. Blucher.

Hildreth, C. (1957). A quadratic programming procedure. *Naval Research Logistics Quarterly*, 4, 79–85.

Li, S., Li, K., Rajamani, R., and Wang, J. (2011). Model predictive multi-objective vehicular adaptive cruise control. *IEEE Transactions on Control Systems Technology*, 19(3), 556–566.

Marsden, G., McDonald, M., and Brackstone, M. (2001). Towards an understanding of adaptive cruise control. *Transportation Research Part C: Emerging Technologies*, 9(1), 33–51.

Michael, P.G., Leeming, F.C., and Dwyer, W.O. (2000). Headway on urban streets: observational data and an intervention to decrease tailgating. *Transportation Research Part F: Traffic Psychology and Behaviour*, 3(2), 55–64.

Naus, G., Ploeg, J., de Molengraft, M.V., Heemels, W., and Steinbuch, M. (2010). Design and implementation of parameterized adaptive cruise control: An explicit model predictive control approach. *Control Engineering Practice*, 18(8), 882–892.

Slotine, J.J.E. and Li, W. (1991). *Applied Nonlinear Control*. Prentice Hall.

Vogel, K. (2003). A comparison of headway and time to collision as safety indicators. *Accident Analysis Prevention*, 35(3), 427–433.

Appendix A. PROOF FOR THE PROPOSITION 1

Proof. Let us use the following literature result. If there are $c_1 \geq 0$, $c_2 \geq 0$, $c_V \geq 0$ that satisfy (A.1) and (A.2), then V leads exponentially stabilizing control Lyapunov function (ESCLF) according to Ames et al. (2017) and Chinelato et al. (2023). That is, a feasible CLF $\forall u \in \mathcal{U}$.

$$c_1||v_h||^2 \geq V(v_h) \geq c_2||v_h||^2 \tag{A.1}$$

$$L_f V(v_h) + L_g V(v_h)u + c_V V(v_h) \leq 0 \tag{A.2}$$

The condition (A.1) is satisfied for $c_1 = c_2 = 1$ since (10) implies $V(v_h) = ||v_h||^2$. The gradient is

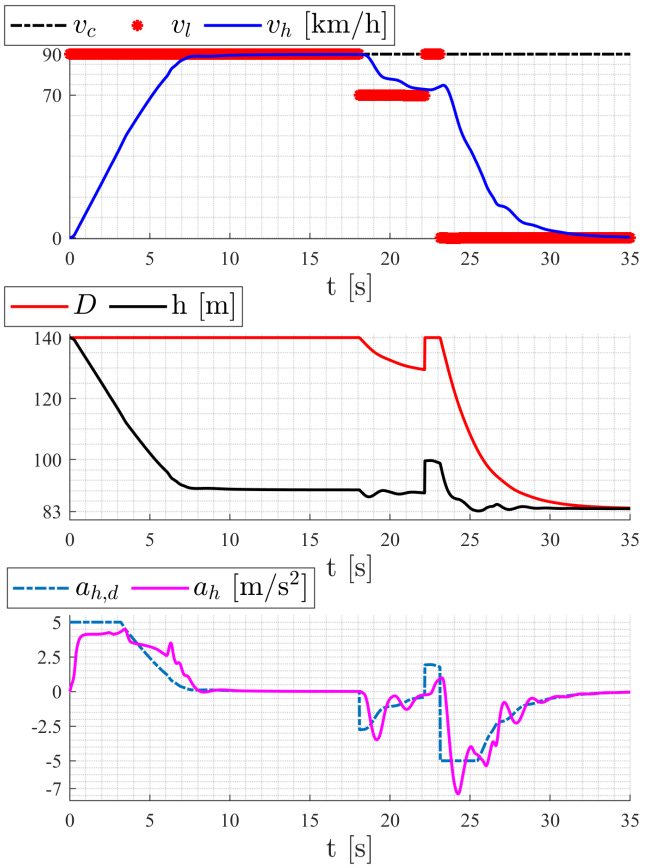

Figure 11. CUT-OUT: Accelerations.

$\nabla V(v_h) = [\frac{\partial V}{\partial v_h}] = [2(v_h - v_c)]$. The Lie derivatives are $L_f V(v_h) = f(v_h)\nabla V(v_h) = \frac{-2(v_h - v_c)F_r(v_h)}{M}$ and $LgV(v_h) = g(v_h)\nabla V(v_h) = 2(v_h - v_c)$. In the case of ACC, $v_h \geq 0$, $F_r(v_h) \geq 0$, $M > 0$, $c_V > 0$. Defining error $e = v_h - v_c$ and $\sigma = \frac{2F_r(v_h)}{M} \geq 0$ condition (A.2) results

$$-\sigma e + 2eu + c_V e^2 \leq 0 \tag{A.3}$$

In case of $e > 0$, rearranging (A.3) and considering the maximum breaking in [m/s^2] as $u^{\min} \leq 0$ the Equation (A.3) implies (A.4).

$$u^{\min} \leq u \leq \frac{\sigma}{2} - \frac{c_V e}{2} \tag{A.4}$$

In case of $e < 0$, rearranging (A.3) and considering the maximum acceleration in [m/s^2] as $u^{\max} \geq 0$ the Equation (A.3) implies (A.5).

$$\frac{\sigma}{2} - \frac{c_V e}{2} \leq u \leq u^{\max} \tag{A.5}$$

In the case of $e = 0$, no control constraint could be obtained from (A.3). An ideal choice should be $u = 0$ but since the model (2) assumes losses such as friction and drag in the form of $F_r(v_h)$, in practice, a small amount of positive control is then required to compensate for these losses and maintain the desired speed, resulting in the $e = 0$ condition.

Looking at (A.4) and (A.5) one can see that the choice of c_V will force the control effort to the limits $u^{\min}$ or $u^{\max}$ depending on the signal of the error.

Understanding the meaning of c_V, it is necessary to find the range C_R, such as $c_V \in C_R$ implies (A.2). From (A.4), the larger error expected for a driver who obeys the law is $e = v^{\max}_{\text{allowed}}$. From (A.4), $e = -v^{\max}_{\text{allowed}}$. Thus, the limits of a parameter c_V such as (A.2) will be respected $\forall u \in \mathcal{U}$ are $c_V^A = \frac{\sigma}{v^{\max}_{\text{allowed}}} - \frac{2u^{\min}}{v^{\max}_{\text{allowed}}}$ and $c_V^B = -\frac{\sigma}{v^{\max}_{\text{allowed}}} + \frac{2u^{\max}}{v^{\max}_{\text{allowed}}}$. Then defining $C_R = [\min(c_V^A, c_V^B), \max(c_V^A, c_V^B)]$ implies (A.2) and consequently the proposition 2. □

Appendix B. PROOF FOR THE PROPOSITION 2

Proof. According to the conditions summarized by Chinelato et al. (2023) first shown by Ames et al. (2017), the $h(x)$ is ZCBF if condition (B.1) was verified for $\gamma > 0$ and $u \in \mathcal{U}$. Note that $\alpha_h(h(x)) = \gamma h(x)$ is an extended class k function (Ames et al., 2017). In other words, it is necessary to prove that there is a non-empty set Γ in which element $\gamma \in \Gamma$ meets the condition (B.1).

$$\sup_{u \in \mathcal{U}} [L_f h(x) + L_g h(x) u + \gamma h(x)] \geq 0 \ , \ \gamma > 0 \tag{B.1}$$

The gradient is $\nabla h(x) = \left[\frac{\partial h(x)}{\partial v_h}, \frac{\partial h(x)}{\partial D}\right] = [-T_d, 1]$. The Lie derivatives are $L_f h(x) = f(x)\nabla h(x) = \frac{T_d F_r(v_h)}{M} + v_\ell - v_h$ and $L_g h(x) = g(x)\nabla h(x) = -T_d$. Isolating u in (B.1)

$$u \leq \underbrace{\frac{\gamma h}{T_d} + \frac{1}{T_d}(v_\ell - v_h) + \frac{F_r(v_h)}{M}}_{\text{ZCBF Condition}} \tag{B.2}$$

The inequality (B.2) implies (B.3). The formulation (B.3) means that ZCBF condition could force breaking ($u = u^{\min}$) when the host travels on the road at the maximum allowed speed $v_h^{\max}$ and the leader is stopped at a minimum distance. And it also means that ZCBF condition could force limited acceleration compared to maximum capacity ($u = \text{ZCBF Condition} < u^{\max}$) when using maximum acceleration leads to unsafe scenario according to ZCBF description (4). And in terms of γ, it can be verified that $\frac{\gamma h}{T_d} > 0$ if there is no accident and then a small γ choice leads to force $u = u^{\min}$ more often compared to a large one.

$$u^{\min} \leq u \leq \text{ZCBF Condition} \leq u^{\max} \tag{B.3}$$

The critical case to be considered is when the host is traveling at $v_h^{\max}$ and the leader is stopped $v_\ell = 0$ at a minimum relative distance $D^{\min}$ defined by the host breaking capacity condition (18). For this situation, the host must break at maximum capacity ($u = u^{\min}$) to maintain safety. Substituting these values on (B.2) leads to (B.4).

$$u^{\min} = \frac{\gamma^{\max}(D^{\min} - T_d v_h^{\max})}{T_d} - \frac{v_h^{\max}}{T_d} + \frac{F_r(v_h^{\max})}{M} \tag{B.4}$$

Now it is clear that the set $\Gamma = \{0 < \gamma < \gamma^{\max}\}$ is not empty and (B.1) is granted for $\forall u \in \mathcal{U}$, $\gamma \in \Gamma$. Thus the forward invariance of the set $\mathcal{C}$ is guaranteed (Ames et al., 2017), that is, (3) is maintained $\forall t \geq 0$ given $x(t = 0) \in \mathcal{C}$ where $t = 0$ is the instant ACC algorithm is initiated. Therefore, the host vehicle never collides with the leader vehicle and proposition 1 is proved. □